



# Production of PLA fibers with surface modifications and silver nanoparticle coating to impart antibacterial activity

Marziyeh Ranjbar Mohammadi<sup>1</sup> · Elham Naghashzargar<sup>1</sup> ·  
Meghdad Kamali Moghaddam<sup>1</sup> · Reza Khorshidi<sup>1</sup>

Received: 22 February 2023 / Revised: 2 August 2023 / Accepted: 30 August 2023 /  
Published online: 11 September 2023

© The Author(s), under exclusive licence to Springer-Verlag GmbH Germany, part of Springer Nature 2023

## Abstract

Infections related to biomedical devices and materials remain a critical healthcare concern, leading to considerable morbidity and disease burden. To combat this issue, the development of fibers with inherent antibacterial properties has garnered significant interest. These fibers offer a large surface area, making them ideal candidates for effective treatment with antibacterial agents. In this study, we present a straightforward procedure for applying silver nanoparticles (AgNPs) to hydrophobic polylactic acid (PLA) fibers that have been surface-modified using sodium hydroxide (NaOH). The method involved electrospinning to create a high-thickness web of PLA fibers, followed by gradual surface modification with NaOH at two different concentrations (0.5 M and 1 M). To confer antibacterial properties to the modified surface samples, we applied silver nanoparticles (AgNPs) at a concentration of 25 mM. In contrast to regular PLA fibers, the surfaces of hydrolyzed PLA (PLA-H) fibers, AgNPs-treated PLA (PLA-A), and hydrolyzed-AgNPs coated PLA (PLA-H-A) fibers exhibited a non-uniform and highly porous structure. EDX analysis provided crucial information about the presence and integration of Ag nanoparticles into the PLA fibers. The PLA-H-A sample exhibited the highest hydrophilicity, with a contact angle of 65.7°. Additionally, the results from differential scanning calorimetry indicated an increase in PLA-H-A's glass transition temperature. Notably, in the Gram-positive *Escherichia coli* (*E. coli*) and Gram-negative *Staphylococcus aureus* (*S. aureus*) tests, the PLA-H-A samples demonstrated highly effective antibacterial properties, effectively preventing bacterial growth.

**Keywords** Surface modification · PLA fibers · Antibacterial · Silver nanoparticles · Hydrophilicity

## Introduction

Electrospinning has rapidly become a leading technique for the production of three-dimensional fibers. In recent years, this method has undergone significant advancements, resulting in extensive research showcasing the successful fabrication of micro and nanofibers through electrospinning [1]. Electrospun fibers were exploited in multidisciplinary fields with numerous applications for decades [2–4]. Porous fibrous materials have gained significant attention in various research fields due to their unique interconnected ultrafine fibrous structure, high specific surface area, permeability, and remarkable plasticity. These materials offer additional advantages such as lightweight nature and versatile applications, making them extensively utilized in numerous research areas [4]. Electrospun fibrous materials, produced using the electrospinning method, possess excellent characteristics that make them highly suitable for biomedical applications. Their ability to manipulate nanofiber components allows for tailoring the materials to achieve desired properties and functions, making them a promising choice in the field of biomedicine [4]. The hydrophobic nature of biodegradable electrospun synthetic polymeric materials, such as polylactic acid (PLA), presents a significant challenge in medical applications. This inherent hydrophobicity can lead to difficulties with cell functions and interactions, limiting their optimal performance in biomedical settings [5]. Enhancing the hydrophilicity of electrospun nanofibers can significantly elevate their performance in applications involving aqueous media. This improvement in hydrophilicity opens doors to a wide range of biomedical applications, including the development of advanced medical devices, tissue engineering scaffolds, and biosensors [6]. Achieving better surface wetting also translates into notable enhancements in material biocompatibility and functionality [7]. In recent times, numerous materials and fabrication techniques have been reported, focusing on the targeted design and enhancement of hydrophilicity for electrospun biodegradable polymer surfaces [8, 9].

Surface modification methods can be categorized into two main groups: permanent and non-permanent methods, or alternatively, into chemical and physical approaches [10]. In chemical approaches, surface modification involves chemical functionalization and covalent grafting, which lead to the formation of new bonds. On the other hand, physical methods involve physical adsorption without forming new chemical bonds. Several permanent surface modification methods have been proposed for PLA, such as atomic transfer polymerization, photografting using UV light, plasma treatment, alkaline surface hydrolysis, and chemical reactions after plasma treatment. These techniques offer promising ways to tailor the surface properties of PLA for various biomedical applications [10, 11]. Plasma and photo-inductive grafting are usually performed under certain critical conditions that may change the properties of the polymer [11]. Alkaline hydrolysis stands out as a simple and cost-effective method for surface modification of PLA. This process specifically targets the ester linkages in the polymer's main chains. Through the dissociation of these ester bonds, carboxylic ( $-\text{COOH}$ ) and hydroxyl end groups ( $-\text{OH}$ ) are formed on the polymer chain, leading to a

reduction in the molecular weight of the modified polymer. This straightforward approach offers an efficient means to tailor the surface properties of PLA for various applications in a cost-effective manner (Fig. 1) [12].

In alkaline hydrolysis containing hydroxide ions (OH<sup>-</sup>), surface modification is more common than volumetric hydrolysis. For volumetric hydrolysis to occur, hydroxide ions must successfully penetrate into the polymer matrix. However, two factors hinder the penetration of hydroxide ions into the polymer: (a) electrostatic repulsion between negatively charged end groups and hydroxide ions, and (b) the bulkier nature of hydroxide ions compared to hydrogen ions. Nevertheless, in cases where the polymer structure is porous, the penetration of hydroxide ions becomes easier, facilitating volumetric hydrolysis. This distinction between surface and volumetric hydrolysis provides insights into how alkaline hydrolysis can selectively modify the polymer surface and how porosity can influence the hydrolysis process. The findings show that the alkaline hydrolysis of the film layer [13], microspheres [14, 15], nanofibrous scaffolds [11, 16, 17] and 3D printed [10, 12] of the polymer with sodium hydroxide has been investigated at different concentrations, temperatures, and times, and the results indicate that the operating conditions depend on the type of substrate used.

Fibers possessing antibacterial activity hold immense significance, considering the widespread bacterial resistance exhibited by many pathogens. Among the approaches to create such fibers, electrospinning stands out as an attractive technique for fabricating composite polymeric fibers with inherent antibacterial properties. This can be achieved through either coating or incorporating well-defined antibacterial nanoparticles. Silver nanoparticles, in particular, are widely acknowledged for their exceptional antibacterial properties, demonstrating a broad spectrum of antibacterial activity. Hence, their utilization in creating antibacterial nanocomposite fibers using electrospinning has garnered significant attention. By developing fibers with inherent antibacterial properties, we can potentially combat bacterial resistance and enhance the efficacy of various biomedical applications, ranging from wound dressings to medical devices. The versatility of electrospinning, coupled with the remarkable antibacterial capabilities of silver nanoparticles, makes this combination a promising avenue for addressing the challenges posed by bacterial infections in healthcare and beyond [18, 19]. This study presents, for the first time in the literature, a novel approach to modify the surface of PLA fibers fabricated by electrospinning followed by the coating of silver nanoparticles onto the hydrolyzed structures. Surface modification was employed to increase the hydrophilicity of PLA, enhancing its interaction with other materials. The alkaline hydrolysis process

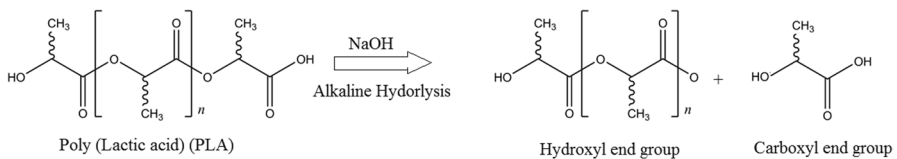


**Fig. 1** The alkaline hydrolysis of ester bond (C–O–C) in PLA

effectively cleaved the ester functional groups on PLA chains, leading to the formation of –OH and –COOH groups on the PLA surface, accompanied by a controlled level of polymer degradation. This homogenous arrangement of silver nanoparticles led to a significant enhancement in the antibacterial property of the fibers. The combined approach of surface modification and silver nanoparticle coating holds great promise for creating advanced antibacterial materials with improved biocompatibility and functionality. This innovative technique has the potential to find applications in various biomedical fields, such as wound dressings, medical devices, and tissue engineering scaffolds, where the control of bacterial growth is of utmost importance.

## Materials and methods

### Materials

In this study, we utilized Polylactic Acid (PLA) type D3251 manufactured by NatureWorks USA, with Mn (Number-average molecular weight) and Mw (Weight-average molecular weight) values of 29,000 g/mol and 52,000 g/mol, respectively. For dissolving the polylactic acid, we employed Dichloromethane (DCM) with a purity of 98%. Furthermore, we incorporated Silver nanoparticles (AgNPs) into the system, procured from U.S. nano company, with a particle size ranging from 80 to 100 nm and a purity of 99.99%. By using these specific materials, we aimed to ensure the quality and consistency of our experimental setup, providing reliable results for our investigation.

### Experiments

To produce PLA fibers, 10% (W/V) polymeric solution in dichloromethane as solvent was prepared 24 h at 25 °C. Then the solution was injected into a 10 ml syringe, and it was spun at a spinning distance of 140 mm (the distance between the nozzle and the collector roller), at an applied voltage of 15 kV and, at feeding rate of 1 mL/h for 8 h [20]. The fabricated fibers in the form of interconnected web were gathered on the rotary collector with a diameter of 5 cm and the rotation speed of 250 rpm. In order to choose the best sample with the smallest contact angle, we performed hydrolysis in two concentrations of sodium hydroxide (0.5 and 1 M) for the time points of 2, 3 and 4 h. After the test period, the hydrolyzed PLA samples (PLA-H) were checked, and the structures that had the least damage in terms of appearance were used to continue the experiments. Then the solution needed to perform the treatment test with silver was prepared. The amount of prepared solution was about 10 cc, which included 8.8 cc of pure ethanol, 0.2 cc of distilled water, and 1 cc of ethylene glycol. Then 0.03 g of 25 mM silver was added to the solution, and it was placed on the stirrer for 30 min until the silver was completely dispersed. Then the PLA-H and PLA fibers were thrown into the prepared solutions and subjected to sonication. After the end of the time, the silver coated PLA and PLA-H fibers (PLA-A and PLA-H-A, respectively) are taken out of the solution and washed with

**Table 1** Description of samples

No	Code	Description
1	PLA	Electrospun polylactic acid
2	PLA-A	AgNPs-treated electrospun polylactic acid
3	PLA-H	Hydrolyzed electrospun polylactic acid
4	PLA-H-A	Hydrolyzed-AgNPs coated electrospun polylactic acid

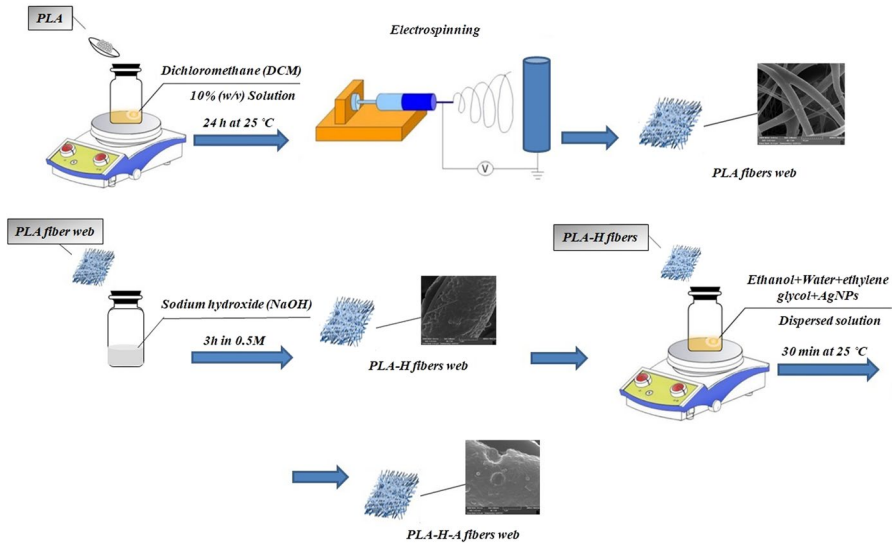


**Fig. 2** Schematic representation of production process of PLA-H-A sample

distilled water three times, then they are placed in the dryer at a temperature of 30° so that the silver is completely fixed on the fiber [21]. Then, we used the contact angle test to check whether the hydrolyzed and silver-treated samples had changed in hydrophilicity or not. For this purpose, four samples, including PLA, PLA-A, PLA-H and PLA-H-A were evaluated (Table 1). Also, the schematic representation of production process of samples is shown in Fig. 2.

### Characterization

The morphology of the fibers was observed using scanning electron microscopy (SEM) (Hitachi, Model S- 4160) at an accelerating voltage of 30 kV, and the average fiber diameter was calculated using microstructure measurement software.

To investigate the chemical properties of various samples, fourier transform infrared spectroscopy (FTIR) analysis (Thermo Nicolet, Nexus 670 made in USA) was used. Thermal properties were assessed by differential scanning calorimetry (model

2010, USA) and samples were heated from 0 to 300 °C at a heating rate of 10 °C/min under an N<sub>2</sub> atmosphere.

For testing the wettability characteristic of samples, a sessile drop method was adopted in which deionized water was automatically dropped on the surface of the fibrous specimens (1\*1 cm<sup>2</sup>). The image of the drop shape on the surface of fibers was taken by video equipment model CAG10 9610IL58300 made by JIKAN CAG 10 Company, and the contact angles were reported using Image J Software.

The antibacterial test against the Gram-negative bacteria *Escherichia coli* (*E. coli* ATCC 25922) and the Gram-positive *Staphylococcus aureus* (*S. aureus* ATCC 29213) was carried out by the Kirby-Bauer method. For this test, areas of clear media surrounding samples indicate that the structure inhibits bacterial growth. After isolating the bacteria, suspensions containing (1 × 10<sup>6</sup> CFU/mL) colonies of *E. coli* and *S. aureus* were prepared and cultured on the surface of a Mueller Hinton Agar plate. The fibers were placed on the surface of the culture medium and then subsequently incubated at 37 °C for 24 h. After incubation time, the diameter of the inhibition zone around the fibers was measured three times by the caliper, and the mean diameter of the inhibition zone was reported.

## Results and discussion

In this research, silver nanoparticles were used as an antimicrobial agent for PLA fibers. The fabricated fibers were surface-modified with alkali, and then silver nanoparticles were placed on the modified and unmodified fibers. Finally, the properties of the samples were investigated.

### Surface modification of fibers

Most of the electrospun fibers from synthetic polymers are relatively hydrophobic, which is undesirable for tissue engineering or other medical applications, and for this reason, they require surface modification. For example, aliphatic polyesters such as PLA show a contact angle in the range of 116–135°, while for the use of structures produced in tissue engineering, the contact angle should be below 100°. The use of strong alkalis can also destroy PLA, but this issue can be prevented by using a mixture of ethanol and sodium hydroxide (NaOH). Therefore, lower concentration of NaOH were used to modify the surface of PLA fibers. After surface hydrolysis, functional hydrophilic groups such as carboxyl and hydroxyl can be created by cutting the ester bond on the surface of PLA fibers [14].

In this study, the surface hydrolysis of fibers using two different concentrations of NaOH (0.5 and 1 M) was done. For each of the concentrations of NaOH, the samples were processed three times (2, 3, and 4 h). The treated samples with 0.5 M NaOH for 2 and 3 h and 1 M for 2 h, did not dissolve, and they were analyzed by contact angle test to find optimized structure. The hydrolyzed sample treated with 0.5 M NaOH for 3 h exhibited a lower contact angle and selected for further experiments. Mohed et al. investigated the surface modification of PLA, in the presence of

**Table 2** The behavior of samples with different concentrations of NaOH and times

Time (h)	NaOH Concentration			
	0.5 M		1 M	
	Behavior in solution	Contact angle	Behavior in solution	Contact angle
2	Not dissolved	85	Not dissolved	84
3	Not dissolved	80	Dissolved	–
4	Dissolved	–	Dissolved	–

**Fig. 3** Dissolved sample in presence of NaOH



different concentrations of NaOH (0.005, 0.3 and 0.5 M) over a period of 50 s. The results showed that the hydrophilicity of PLA increased in the presence of NaOH, and also that the hydrophilicity of PLA with a half molar sodium hydroxide concentration is greater than 0.3 and 0.05 molar sodium hydroxide [22]. Table 2 displays the obtained results. Also, Fig. 3 is the image of the dissolved sample. The other investigation showed that after 48 h and at a concentration of 3 M and higher NaOH, the alkaline hydrolysis process causes the complete dissolution of the PLA scaffold, while at lower concentrations and in a shorter time, the scaffold remains unchanged even though it is affected by the hydrolysis process [12] (Table 2).

**SEM structures of samples**

The SEM images of the manufactured fibers are shown in Fig. 4. PLA fibers with an average diameter of  $851 \pm 100$  nm exhibited a smooth structure without any cracks or bead. After the alkaline hydrolysis of PLA by sodium hydroxide, due to the bonding of sodium hydroxide with PLA and the breaking of ester bonds, surface roughness can be seen in the structure of the fibers [14, 22]. The application of dichloromethane as a solvent in the production of the fibers, which has a high volatility, has caused the creation of a porous structure in the fibers, which is due to the evaporation of dichloromethane and the production of porosity. But as can be seen, in the PLA-H sample, the pores appear more clearly on the surface of the sample,



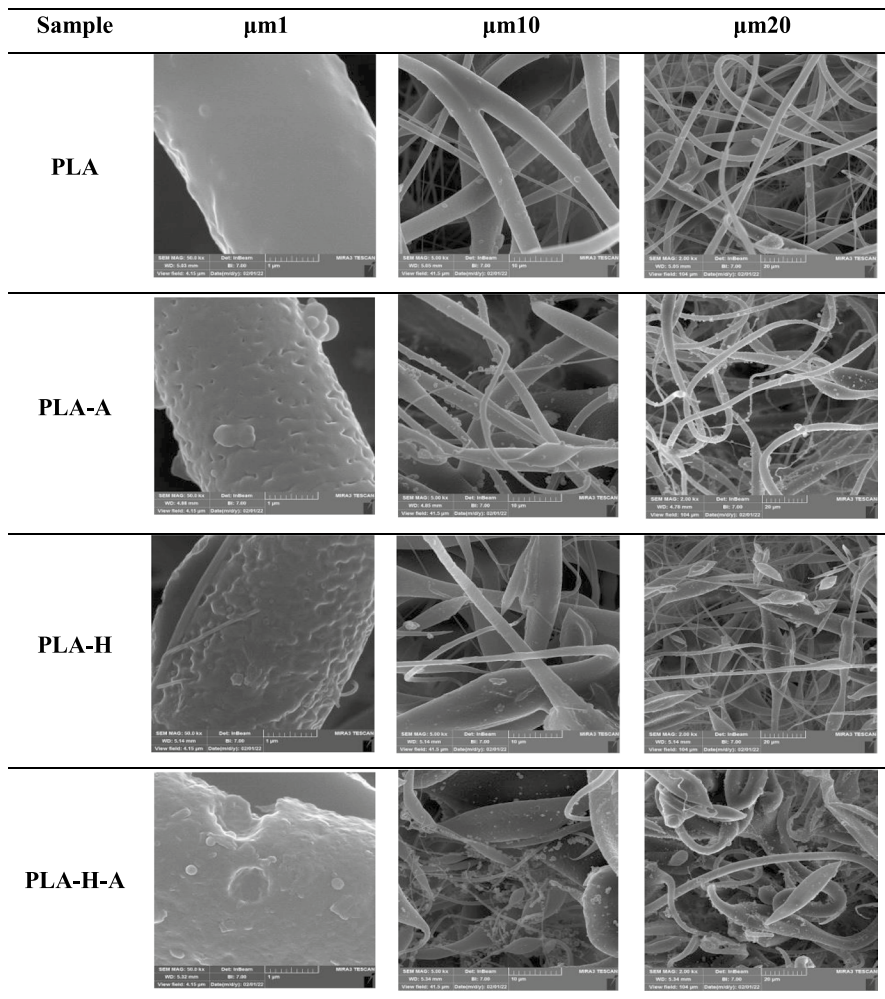


**Fig. 4** SEM images of fabricated samples

and this indicates the introduction of alkali into the fiber and changes in the fiber morphology.

For the PLA-A sample as well as the PLA-H-A sample, silver nanoparticles were dispersed on the surface of the PLA fibers. The surface of PLA-A fibers is almost smooth and uniform like that of PLA fibers, and the depth of pores is not as great as in hydrolyzed samples [23].

According to Fig. 4 for the PLA-H-A sample, silver nanoparticles can be seen at all the points of the fibers. Also, due to alkaline hydrolysis by NaOH, a porous structure with surface roughness was observed [24]. In addition, it appears that more nanoparticles are spread on the surface of the fibers in PLA-H-A samples than in the PLA-A sample. From the SEM results obtained in this research, we have also



proposed that the mechanism of alkaline hydrolysis on PLA-H and PLA-H-A was in surface erosion mode.

After measuring the average diameter of the fibers, no significant change was observed in the average diameter of fibers, and the diameter of PLA-H, PLA-H-A, and PLA-A fibers was about  $830 \pm 120$ ,  $820 \pm 110$ , and  $800 \pm 99$  nm, respectively. The reason for this could be that the changes and operations performed on the fibers happened after they were manufactured, so the entire operation performed on the fibers had no effect on the average diameter of fibers.

EDX analysis is a valuable tool for identifying the elemental composition and distribution of PLA and Ag nanoparticles in both PLA-H and PLA fibers. The presence of Ag nanoparticles in the PLA samples was successfully detected through EDX analysis, confirming their incorporation into both PLA-H and PLA structures.

Table 3 and Fig. 5 further support the presence of Ag nanoparticles in the PLA and PLA-H structures. As expected, the specific elements of PLA, carbon (C), and oxygen (O), were found in all samples. In the PLA-H sample, the elemental composition showed approximately 69.27% carbon and 30.70% oxygen. Additionally, the high percentage of Ag element detected in the PLA-H sample through EDX analysis confirms the successful incorporation of silver nanoparticles in the fiber structure. This indicates a successful modification process, resulting in higher silver content in the fibers. Furthermore, EDX map images (Fig. 5) provided visual evidence of Ag distribution on the PLA nanofibrous webs, further supporting the effective integration of Ag nanoparticles into the fibers. Overall, the EDX analysis provides robust evidence for the successful incorporation of Ag nanoparticles into the PLA-H and PLA fibers, validating the surface modification and reinforcing the potential of these nanofibrous materials for various applications, particularly in areas where antibacterial properties are essential.

### Hydrophilicity nature of the fibers

One of the most crucial properties of scaffolds for use in tissue engineering is their unique affinity for water. Compared to hydrophobic structures, which have few functional groups that can interact with cells, nanofibers with hydrophilic nature increase the cellular functions like cell adhesion and proliferation. The hydrophilicity or hydrophobicity of nanofibrous structure can be determined by measuring its contact angle with a water droplet [25]. In high hydrophilic and low hydrophilic surfaces, the contact angle between the water drop and the surface is approximately  $0\text{--}30^\circ$

**Table 3** Elemental composition of PLA-H, PLA-A and PLA-H-A samples by EDX

Samples	Elemental composition (%)		
	C	O	Ag
PLA-H	69.27	30.73	0
PLA-A	62.32	31.95	5.73
PLA-H-A	57.57	5.73	18.50

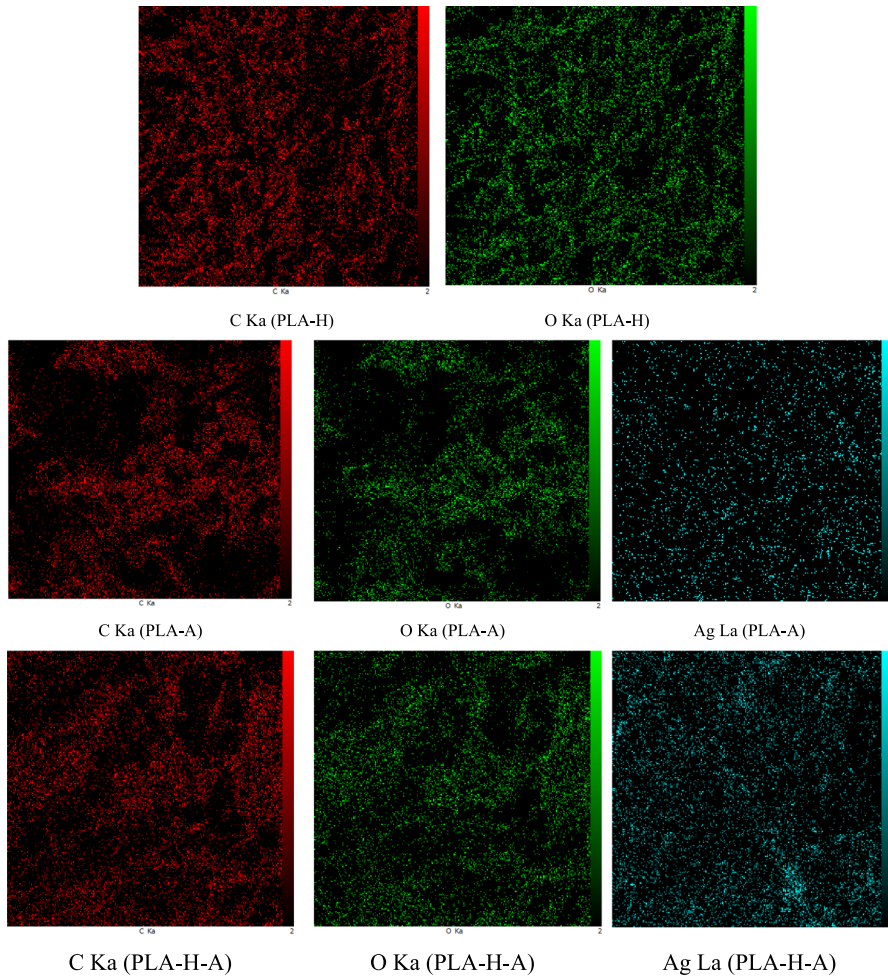


**Fig. 5** EDX maps of PLA, PLA-A and PLA-H-A nanofibrous webs shown Ag elements

**Table 4** Calculated contact angle for different samples

Samples	3 s	6 s	9 s	Average
PLA	125.6	120.2	105.7	117.17
PLA-A	122.3	119.0	103.1	114.8
PLA-H	88.2	82.7	79.3	83.4
PLA-H-A	70.123	67.789	59.421	65.77

and 30–90°, respectively. If the contact angle is more than 90°, the structure can be classified as hydrophobic [26].

The measured contact angles at three time points of 3, 6, and 9 s for four samples are shown in the Table 4 and Fig. 6. The smaller the contact angle and

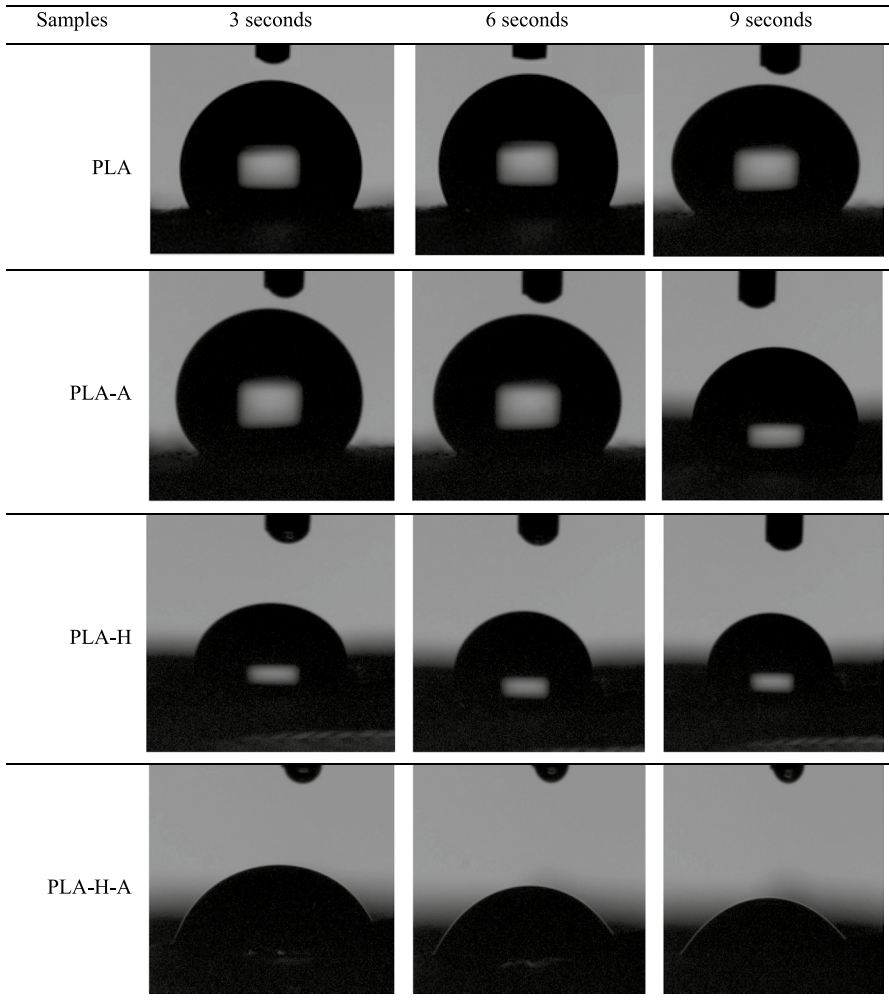


**Fig. 6** Captured contact angle image for different samples

the closer it is to zero, the claim can be made that the sample is more hydrophilic. After measuring the contact angle, it can be seen that the contact angle of PLA-H has decreased compared to the PLA sample, which indicates that it is more hydrophilic [14]. Also, the contact angle of the PLA-A sample is somewhat lower than that of PLA, which indicates the improvement in the hydrophilic properties of this sample. So it can be concluded that the contact angle of PLA-H-A is lower than other samples, which shows that this structure is more hydrophilic. The results of this section confirms the findings of other studies [27, 28].

## FTIR results

In this research, infrared spectroscopy (FTIR) was used in order to identify the functional groups, investigate about the chemical interactions and possible structural changes in the blended polymers during the process of preparing electrospinning solutions. The analysis of PLA, PLA-A, PLA-H and PLA-A-H samples is shown in Fig. 7. For PLA sample, the peaks at 2993 and 2943  $\text{cm}^{-1}$  indicate the asymmetric stretching vibration of  $\text{CH}_2$  groups in PLA structure. Also, a strong and broad peak can be seen at the wavenumber 1710  $\text{cm}^{-1}$ , which is related to the  $\text{C}=\text{O}$  stretching vibrations of PLA. The observed peak at wavenumbers of 1450 and 1358  $\text{cm}^{-1}$  represent the stretching vibration of the  $\text{CH}_3$  group in PLA. Also, the peak related to the stretching of the ester group ( $\text{C}-\text{O}-\text{C}$ ) can be seen at the wavenumber of 1079  $\text{cm}^{-1}$ . Finally, the peaks related to  $\text{C}-\text{CH}_3$  and  $\text{C}-\text{COO}$  stretching can also be visible at 1039 and 865  $\text{cm}^{-1}$ .

For the PLA-H sample, the peaks related to  $\text{CH}_2$ ,  $\text{C}=\text{O}$ ,  $\text{CH}_3$ ,  $\text{C}-\text{O}$  and,  $\text{C}-\text{O}-\text{C}$ ,  $\text{C}-\text{CH}_3$  and  $\text{C}-\text{COO}$  stretching mode are observable at wavenumbers of 2993 and 2943, 1708, 1450 and 1350, 1179, 1078, 1038 and 865  $\text{cm}^{-1}$ , respectively. Among the available peaks for the sample of PLA-H, the wavenumber of the peak related to the carbonyl group shifted to lower numbers. In addition, another very weak peak can be seen at 3300 and 3600  $\text{cm}^{-1}$ , which is related to the creation of hydroxyl group ( $\text{OH}$ ) on the surface of PLA fibers in the result of hydrolysis process. Manzhou et al. investigated the effect of  $\text{NaOH}$  on the  $\text{ZnO}$  incorporated PLA nanofibers. The FTIR results for PLA-H in their study showed that the peak observed at the wavenumber 3430  $\text{cm}^{-1}$

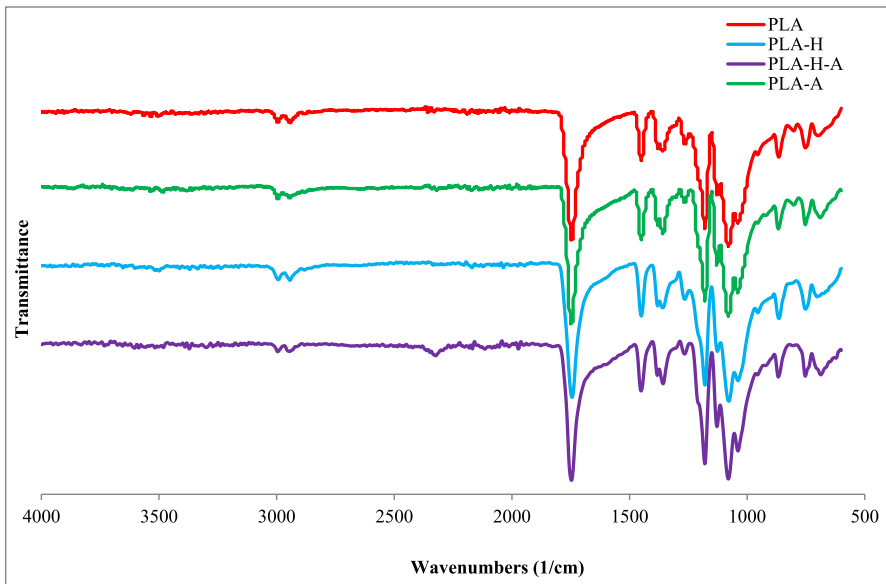


Fig. 7 FTIR results for different samples

was representative of the stretching vibration of the hydroxyl group (OH) and the peak observed at  $1750\text{ cm}^{-1}$  was related to the stretching mode of the carbonyl group [29]. Also, Schneider et al. performed alkaline hydrolysis by sodium hydroxide on PLA 3D printing scaffolds, and the wavenumbers corresponding to the stretching peaks of OH, C=O, C–O, C–C, CH<sub>3</sub>, CH<sub>2</sub> were 3300 and 3500 were seen at 1748 and 1452, 1180, 869, 1453, 2995 and  $2945\text{ cm}^{-1}$ , respectively [12].

For the PLA-H-A sample, according to the results, the peaks related to CH<sub>2</sub>, C=O, CH<sub>3</sub>, C–O, C–O–C, C–CH<sub>3</sub> and C–COO stretching were shown in wavenumbers of 2995 and 2945, 1750, 1451 and 1357, 1180, 1080, 1039,  $867\text{ cm}^{-1}$ , respectively. Compared to the peaks of PLA, the wavenumbers of the peaks related to PLA-H-A sample exhibited somewhat shift to higher numbers. Rarima et al. investigated the FTIR results of PLA/silver nanoparticles nanocomposite membrane. In their results, the wavenumbers for the stretching peaks related to OH, CH<sub>2</sub>, C–O, C=O, CH<sub>3</sub> in PLA-H-A sample were observable at 3500, 2994 and 2940, 1175, 1746,  $1453\text{ cm}^{-1}$ , respectively [23]. The interaction between PLA-H and silver occurs in the peak with a wavenumber of  $13,500\text{ cm}^{-1}$ , which is related to the stretching mode of the OH group. Also, all of the peaks for PLA have been preserved after hydrolysis and its mixture with AgNPs.

For the PLA-A sample, the peaks related to the stretching of CH<sub>2</sub>, C=O, CH<sub>3</sub>, C–O, C–O–C, C–CH<sub>3</sub> and C–COO groups are observable in the wavenumbers of 2994 and 2994, 1747, 1450 and 1357, 1180, 1080, 1039 and  $1867\text{ cm}^{-1}$ , respectively. Kumar et al. for PLA/silver nanofibers reported the wavenumbers of stretching peaks for C–O, C–H, C–H, CH<sub>3</sub>, OH, and C=O groups at 1177, 2989, 1452, 1356, 3350 and  $11,751\text{ cm}^{-1}$ , respectively [30].

## DSC results of fabricated samples

DSC analysis was done to check the thermal properties (glass transition temperature and melting temperature) of PLA, PLA-H, PLA-A-H, PLA-A samples, which DSC diagram is shown in Fig. 8. For the PLA sample, an endothermic peak at around  $54\text{--}76\text{ }^{\circ}\text{C}$  corresponds to the glass transition temperature ( $T_g$ ). As temperature is increased, the second endothermic peak is observed at around  $155\text{ }^{\circ}\text{C}$ . This exhibits the melting temperature ( $T_m$ ) of PLA fibers. In the other study of Cao et al., the temperatures corresponding to the  $T_g$  and  $T_m$  of PLA were reported to be  $61.8\text{ }^{\circ}\text{C}$  and  $157\text{ }^{\circ}\text{C}$ , respectively [31]. Their results demonstrated that the  $T_g$  and  $T_m$  of the PLA after blending with poly hydroxyl ester ether decreased [31].

For the PLA-H sample, an endothermic peak was observed at  $58.2\text{ }^{\circ}\text{C}$ , which corresponds to the  $T_g$  of the PLA. Also, another peak can be seen at  $150\text{ }^{\circ}\text{C}$ , which indicates the melting temperature of PLA-H. After hydrolysis of PLA, its melting temperature has shown a decrease. Schneider et al. performed alkaline hydrolysis by NaOH on PLA 3D printing scaffolds and reported  $58\text{ }^{\circ}\text{C}$  and  $146\text{--}154\text{ }^{\circ}\text{C}$  for the  $T_g$  and  $T_m$ , respectively [12]. In the other study, the  $T_g$  and  $T_m$  for hydrolyzed PLA with NaOH was about  $53.94$  and  $152.50\text{ }^{\circ}\text{C}$ , respectively [32].

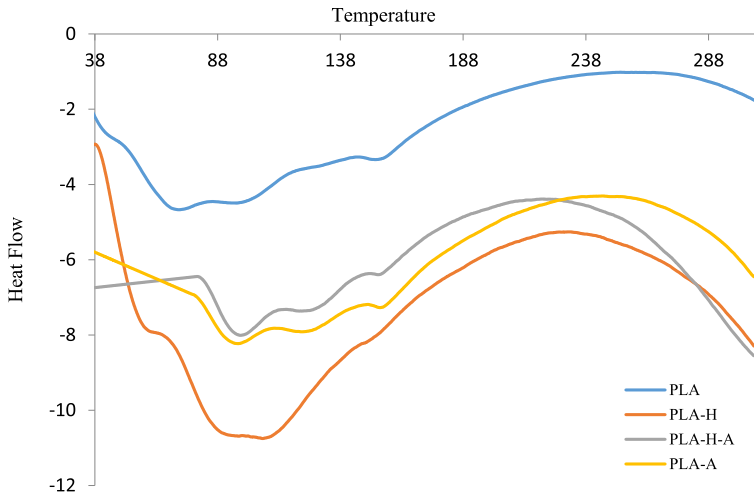


**Fig. 8** DSC thermograms of samples

For the PLA-A sample, an endothermic peak at 61.3 °C has been reported, which indicates the  $T_g$  of this blend. Also, the  $T_m$  of this structure was observable at 155.7 °C. By adding silver nanoparticles to PLA and comparing this structure with PLA and PLA-H samples, the  $T_g$  has shown an increase, according to the obtained results, the melting temperature of PLA-A does not change much compared to the other samples. Fortunati et al. Described the  $T_g$  and  $T_m$  for the PLA-A about 56 and 149.4 °C, respectively [33].

For the PLA-A-H sample, a peak at 62.6 °C has been reported, which corresponds to the the  $T_g$  of this structure. Also, another peak can be seen at 154/96, which demonstrates the  $T_m$  of the PLA-A-H. Compared to the other three samples, PLA-A-H has the highest  $T_g$ . It can also be seen from the obtained results that the  $T_m$  has not changed much.

### Antibacterial analysis

Silver nanoparticles and nanocomposites containing them are considered as widely used nanomaterials in medical and biotechnology applications due to their high antimicrobial efficiency. AgNPs in certain concentrations have high antimicrobial activity that are nontoxic to human cells. Antimicrobial activity of PLA-H-A and PLA-A samples against gram-positive bacteria *S. aureus* and gram-negative bacteria *E.coli* was investigated using agar disk diffusion method (Fig. 9). The diameter of inhibition zone for PLA-A and PLA-H-A samples was about 15 and 30 mm for *E. coli*, respectively and 0 and 15 mm for *S. aureus* bacteria. According to the results, the antimicrobial activity of PLA-H-A sample against gram negative *E. coli* is higher than the antibacterial activity of fibers against gram-positive *S. aureus*, which can be attributed to the difference in the cell wall of the *E. coli*. The cell wall of *E.*



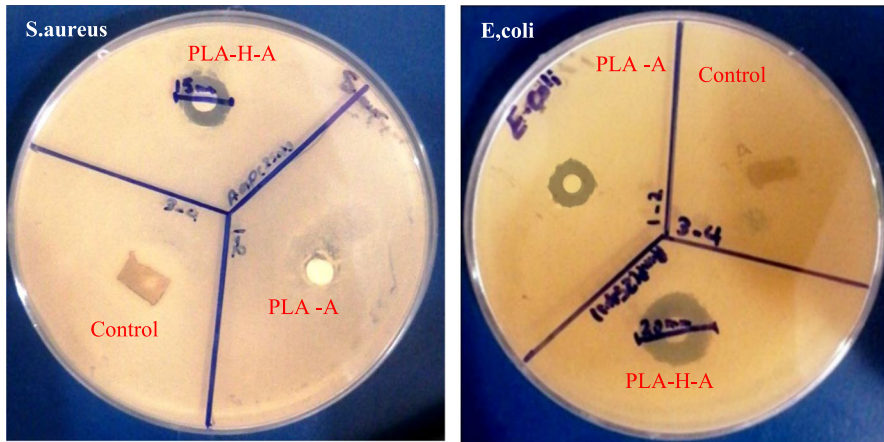


**Fig. 9** Inhibition zone for the PLA-A and PLA-H-A samples

*coli* contains fats, proteins and lipopolysaccharides, which show effective protection against bacteria. While the cell wall of gram-positive *S. aureus* does not have lipopolysaccharide. Also, by increasing the concentration of silver nanoparticles, the antimicrobial activity of the samples increases [34].

## Conclusion

Chronic infections often result from bacterial infections, highlighting the urgent need for antibacterial solutions in clinical settings. In this study, we employed the electrospinning technique to create PLA fibers, and subsequently evaluated their morphology and hydrophilicity.

SEM analysis of the PLA fibers showed a smooth and crack-free surface. However, after hydrolysis and surface modification with NaOH, the morphology became non-homogeneous, and the surface displayed porosity with visible cavities. The addition of silver nanoparticles resulted in even distribution on the fiber surface. In the PLA-H-A sample, the cavity depth reduced compared to PLA-H. The PLA-A structure showed a fractured and beaded surface, contrasting the smooth and uniform surface of pure PLA. Measurements of the fiber diameter revealed minimal variations, indicating that the modifications and procedures applied did not significantly impact the average fiber diameter. EDX results provided crucial information about the presence and integration of Ag nanoparticles into the PLA matrix. Hydrophilicity measurements indicated that samples with lower contact angles exhibited higher hydrophilicity. The PLA-H-A sample demonstrated the lowest contact angle and the highest hydrophilicity among the samples, measuring  $65.7^\circ$ . Surface modification and the incorporation of silver nanoparticles increased the hydrophilicity and reduced the contact angle of the fibers. FTIR analysis confirmed the presence of sodium hydroxide and AgNPs in the structure of the fibers. Thermal analysis of the PLA-H-A sample showed minimal variation in melting temperature-related peaks.



In antibacterial tests, the PLA-H-A sample displayed inhibition zones of 15 mm and 20 mm against *Staphylococcus aureus* and *Escherichia coli* bacteria, respectively. The antibacterial activity of PLA-H-A against both Gram-positive and Gram-negative bacteria was stronger than that of PLA-A. Overall, our findings demonstrate the successful modification of PLA fibers to enhance their hydrophilicity and antibacterial properties, making them promising candidates for biomedical applications where antibacterial efficacy is vital.

**Author contributions** Conceptualization, MRM; Methodology, MRM, MKM; Investigation, RK; Writing-Original Draft Preparation, MRM.; Writing-Review and Editing, MRM, MKM, EN; Supervision, MRM, EN.

**Funding** This research did not receive any specific grant from funding agencies in the public, commercial, or not-for-profit sectors.

**Availability of data and materials** The authors confirm that the data supporting the findings of this study are available within the article.

## Declarations

**Conflict of interest** The authors declare that they have no known competing financial interests or personal relationships.

**Ethical approval** Not applicable.

## References


1. Nirwan VP, Kowalczyk T, Bar J, Buzgo M, Filová E, Fahmi A (2022) Advances in electrospun hybrid nanofibers for biomedical applications. *Nanomaterials* 12(11):1829
2. Ranjbar-Mohammadi M, Yousefi E (2022) Fabrication of a dye removal system through electrospun of TiO<sub>2</sub>/Nylon-6 nanocomposite on three-dimensional spacer fabrics. *Polym Bull* 79(5):2953–2967
3. Ranjbar-Mohammadi M, Bahrami SH, Joghataei M (2013) Fabrication of novel nanofiber scaffolds from gum tragacanth/poly (vinyl alcohol) for wound dressing application: in vitro evaluation and antibacterial properties. *Mater Sci Eng C* 33:4935
4. Shirazi MMA, Kargari A, Ramakrishna S, Doyle J, Rajendrian M, Babu PR (2017) Electrospun membranes for desalination and water/wastewater treatment: a comprehensive review. *J Membr Sci Res* 3:209
5. Agarwal S, Wendorff JH, Greiner A (2010) Chemistry on electrospun polymeric nanofibers: merely routine chemistry or a real challenge? *Macromol Rapid Commun* 31:1317
6. Encinas N, Pantoja M, Abenojar J, Martínez M (2010) Control of wettability of polymers by surface roughness modification. *J Adhes Sci Technol* 24:1869
7. Menzies KL, Jones L (2010) The impact of contact angle on the biocompatibility of biomaterials. *Optom Vis Sci* 87:387
8. Hendrick E, Frey M (2014) Increasing surface hydrophilicity in poly (lactic acid) electrospun fibers by addition of PLA-b-PEG co-polymers. *J Eng Fibers Fabr* 9:155892501400900220
9. Ranjbar-Mohammadi M, Prabhakaran MP, Bahrami SH, Ramakrishna S (2016) Gum tragacanth/poly (l-lactic acid) nanofibrous scaffolds for application in regeneration of peripheral nerve damage. *Carbohydr Polym* 140:104
10. Baran EH, Erbil HY (2019) Surface modification of 3D printed PLA objects by fused deposition modeling: a review. *Colloids Interfaces* 3:43
11. Niemczyk-Soczynska B, Gradyś A, Sajkiewicz P (2020) Hydrophilic surface functionalization of electrospun nanofibrous scaffolds in tissue engineering. *Polymers* 12:2636

12. Schneider M, Fritzsche N, Puciul-Malinowska A, Baliś A, Mostafa A, Bald I, Zapotoczny S, Taubert A (2020) Surface etching of 3D printed poly (lactic acid) with NaOH: a systematic approach. *Polymers* 12:1711
13. Tham CY, Hamid ZAA, Ahmad Z, Hanafi I, In: *Adv Mater Res Ed.^Eds.*, 324, Year of Convergence
14. Tham C, Hamid ZAA, Ahmad Z, Ismail H (2014) Surface engineered poly (lactic acid)(PLA) microspheres by chemical treatment for drug delivery system, *Trans Tech Publ*
15. Trang TTT, Jaafar M, Yahaya BH, Kawashita M, Tram NXT, Hamid ZAA, In: *J Phys: Conf Ser"Ed.^Eds.*, 012068, Year of Convergence
16. Haddad T, Noel S, Liberelle B, El Ayoubi R, Ajjji A, De Crescenzo G (2016) Fabrication and surface modification of poly lactic acid (PLA) scaffolds with epidermal growth factor for neural tissue engineering. *Biomatter* 6:e1231276
17. Yang J, Wan Y, Tu C, Cai Q, Bei J, Wang S (2003) Enhancing the cell affinity of macroporous poly (L-lactide) cell scaffold by a convenient surface modification method. *Polym Int* 52:1892–1899
18. Prasher P, Singh M, Mudila H (2018) Silver nanoparticles as antimicrobial therapeutics: current perspectives and future challenges. *3Biotech* 8:1
19. Rai MK, Deshmukh SD, Ingle AP, Gade AK (2012) Silver nanoparticles: the powerful nanoweapon against multidrug-resistant bacteria. *J Appl Microbiol* 112:841
20. Ranjbar-Mohammadi M, Shakoori P, Arab-Bafrani Z (2021) Design and characterization of keratin/PVA-PLA nanofibers containing hybrids of nanofibrillated chitosan/ZnO nanoparticles. *Int J Biol Macromol* 187:554
21. Gottesman R, Shukla S, Perkas N, Solovyov LA, Nitzan Y, Gedanken A (2011) Sonochemical coating of paper by microbiocidal silver nanoparticles. *Langmuir* 27:720
22. Sabee MM, Kamalaldin N, Yahaya B, Hamid ZA (2016) Characterization and in vitro study of surface modified PLA microspheres treated with NaOH. *J Polym Mater* 33:191
23. Rarima R, Unnikrishnan G (2020) Porous poly (lactic acid)/nano-silver composite membranes for catalytic reduction of 4-nitrophenol. *Mater Chem Phys* 241:122389
24. Xu X, Yang Q, Wang Y, Yu H, Chen X, Jing X (2006) Biodegradable electrospun poly (L-lactide) fibers containing antibacterial silver nanoparticles. *Eur Polym J* 42:2081
25. Oves M, Khan MZ, Ismail IM (2018) *Modern age environmental problems and their remediation*, Springer
26. Haider A, Haider S, Kang I-K (2018) A comprehensive review summarizing the effect of electrospinning parameters and potential applications of nanofibers in biomedical and biotechnology. *Arab J Chem* 11:1165
27. Kim JS, Kuk E, Yu KN, Kim J-H, Park SJ, Lee HJ, Kim SH, Park YK, Park YH, Hwang C-Y (2007) Antimicrobial effects of silver nanoparticles. *Nanomed Nanotechnol Biol Med* 3:95
28. Möhler JS, Sim W, Blaskovich MA, Cooper MA, Ziora ZM (2018) Silver bullets: a new lustre on an old antimicrobial agent. *Biotechnol Adv* 36:1391
29. Liu M, Wang Y, Cheng Z, Song L, Zhang M, Hu M, Li J (2014) Function of NaOH hydrolysis in electrospinning ZnO nanofibers via using polylactide as templates. *Mater Sci Eng: B* 187:89
30. Ramos M, Fortunati E, Peltzer M, Dominici F, Jiménez A, del Carmen Garrigós M, Kenny JM (2014) Influence of thymol and silver nanoparticles on the degradation of poly (lactic acid) based nanocomposites: thermal and morphological properties. *Polym Degrad Stabil* 108:158–165
31. Cao XINGXIANG, Mohamed A, Gordon SH, Willett JL, Sessa DJ (2003) DSC study of biodegradable poly (lactic acid) and poly (hydroxy ester ether) blends. *Thermochim acta* 406:115
32. Wan Jaafar WNR, Siti Norasmah S, Azmi NN, Noor Najmi B, Anuar H, Hassan NA, B. Abdul Razak S, In: *Adv Mater Res Ed.^Eds.*, 342, Year of Convergence
33. Fortunati E, Armentano I, Iannoni A, Kenny J (2010) Development and thermal behaviour of ternary PLA matrix composites. *Polym Degrad Stab* 95:2200
34. Shahverdi AR, Fakhimi A, Shahverdi HR, Minaian S (2007) Nanomedicine: nanotechnology. *Biol Med* 3:168

**Publisher's Note** Springer Nature remains neutral with regard to jurisdictional claims in published maps and institutional affiliations.

Springer Nature or its licensor (e.g. a society or other partner) holds exclusive rights to this article under a publishing agreement with the author(s) or other rightsholder(s); author self-archiving of the accepted manuscript version of this article is solely governed by the terms of such publishing agreement and applicable law.

## Authors and Affiliations

Marziyeh Ranjbar Mohammadi<sup>1</sup>  · Elham Naghashzargar<sup>1</sup> ·  
Meghdad Kamali Moghaddam<sup>1</sup> · Reza Khorshidi<sup>1</sup>

✉ Marziyeh Ranjbar Mohammadi  
m.ranjbar@ubonab.ac.ir

✉ Elham Naghashzargar  
en.zargar@gmail.com

<sup>1</sup> Department of Textile Engineering, Faculty of Engineering, University of Bonab,  
Bonab 5551395133, Iran